PHYSICAL REVIEW D **81,** 054001 (2010)

Fragmentation functions in nuclear media

Rodolfo Sassot*
Instituto de Física de Buenos Aires, CONICET, Departamento de Física, Facultad de Ciencias Exactas y Naturales, Universidad de Buenos Aires, Ciudad Universitaria, Pabellón 1 (1428) Buenos Aires, Argentina

Marco Stratmann†
Institut für Theoretische Physik, Universität Regensburg, 93040 Regensburg, Germany and Institut für Theoretische Physik und Astrophysik, Universität Würzburg, 97074 Würzburg, Germany

Pia Zurita‡
Instituto de Física de Buenos Aires, CONICET, Departamento de Física, Facultad de Ciencias Exactas y Naturales, Universidad de Buenos Aires, Ciudad Universitaria, Pabellon 1 (1428) Buenos Aires, Argentina
(Received 9 December 2009; revised manuscript received 9 February 2010; published 4 March 2010)

We perform a detailed phenomenological analysis of how well hadronization in nuclear environments can be described in terms of effective fragmentation functions. The medium modified fragmentation functions are assumed to factorize from the partonic scattering cross sections and evolve in the hard scale in the same way as the standard or vacuum fragmentation functions. Based on precise data on semi-inclusive deep-inelastic scattering off nuclei and hadron production in deuteron-gold collisions, we extract sets of effective fragmentation functions for pions and kaons at next-to-leading order accuracy. The obtained sets provide a rather accurate description of the kinematical dependence of the analyzed cross sections and are found to differ significantly from standard fragmentation functions both in shape and magnitude. Our results support the notion of factorization and universality in the studied nuclear environments, at least in an effective way and within the precision of the available data.

DOI: 10.1103/PhysRevD.81.054001 PACS numbers: 13.87.Fh, 12.38.Bx, 13.85.Ni

I. INTRODUCTION AND MOTIVATION

In spite of the remarkable phenomenological success of quantum chromodynamics (QCD) as the theory of strong interactions, a detailed quantitative understanding of hadronization processes is still one of the great challenges for the theory. Hadronization is the mechanism by which a final-state quark or gluon, excited in some hard partonic interaction, dresses itself and develops into an observed final-state hadron. As such, it is sensitive to physics happening at long distances and time scales, and perturbative tools that have earned QCD its present standing, simply fall short. On the other hand, studying hadronization process is a path to understand the phenomenon of confinement and opens a window to the nonperturbative domain of QCD.

The last few years have seen a significant improvement in the perturbative QCD (pQCD) description of scattering processes with identified produced hadrons. More specifically, precise determinations of fragmentation functions for various different hadron species have been performed [1–3]. Fragmentation functions parametrize the nonperturbative details of the hadronization process and, by virtue of the factorization theorem, are assumed to be universal, i.e., process independent [4]. One of the most interesting results of these studies is that the standard pQCD framework not only reproduces the data on electron-positron annihilation into hadrons with remarkable precision, but describes equally well other processes, like semi-inclusive deep-inelastic scattering (SIDIS) and hadron production in proton-proton collisions [1]. Using the wealth of data with identified hadrons in a global QCD analysis not only increases the precision and kinematical coverage of fragmentation functions, but more importantly, supports the ideas of factorization and universality in the kinematical domain accessed by these experiments. These concepts are the starting points for the successful pQCD description of hard scattering processes.

For more than 30 years, it has been known that results for hadron production processes occurring in a nuclear environment can differ significantly from similar experiments involving only light nuclei or proton targets [5]. More recently, detailed kinematic distributions for production rates of identified hadrons in SIDIS off different nuclei have been provided by the HERMES experiment [6]. The origin of the observed differences induced by the nuclear media, has been attributed to a variety of conceivable mechanisms besides the well-known modification of parton densities in nuclei. Ideas range from interactions between the nuclear medium and the seed partons before the hadronization takes place, as implemented through pQCD inspired models, to interactions between the medium and the final-state hadrons, usually formulated in a nuclear and hadron physics language; for recent reviews, see Refs. [7,8]. Most models reproduce, with different degrees

*sassot@df.uba.ar
†marco@ribf.riken.jp
‡pia@df.uba.ar

of success, some features of the data, in spite of very different, even orthogonal theoretical approaches and ingredients.

In the case of the so-called initial-state nuclear effects, such as those observed in inclusive deep-inelastic scattering (DIS) off nuclei [9] and the Drell-Yan process on nuclear targets [10], it has been shown that the influence of the nuclear environment can be effectively factorized into a set of modified nuclear parton distribution functions (nPDFs). The nPDFs scale in energy with standard evolution equations, and conventional partonic hard scattering cross sections can be utilized in calculations. Within the precision of the available data, this approach has been demonstrated to be an excellent approximation at next-to-leading order (NLO) accuracy of pQCD, and allows one to continue to exploit the key features of factorization and universality in a nuclear environment [11–13]. From the QCD point of view, the nPDFs carry all the nonperturbative information related to the probed nuclei, just as the standard parton densities parametrize our knowledge of the nucleon. Both need to be obtained in global QCD fits to data or approximated within a given nonperturbative model.

It is quite natural then to ask if the idea of factorization can be extended to final-state nuclear effects and to explore how good such an approximation works in practice or, alternatively, to determine where and why it breaks down. From a theoretical point of view, however, the answer to the question whether the introduction of medium modified fragmentation functions (nFFs) is a viable concept is not obvious. On the one hand, interactions with the nuclear medium may spoil the requirements of factorization theorems and, e.g., induce scale dependent effects different to those expected in the standard Dokshitzer-Gribov-Lipatov-Altarelli-Parisi (DGLAP) framework, as discussed in different proposals [14]. On the other hand, presently available estimates of factorization breaking effects [14] are strongly model dependent and based on tree level calculations.

Assuming that factorization holds, the medium modified fragmentation functions should contain (factorize) all the nonperturbative details relevant for the computation of hard processes with identified hadrons and would be interchangeable from one process to another, i.e., universal. On top of that, such a theoretical framework is well defined, has predictive power, and can be systematically extended beyond the leading order (LO) approximation. The inclusion of higher order QCD corrections and the possibility to use different observables simultaneously in a global analysis have both been proven to be crucial for a successful extraction of vacuum fragmentation functions (FFs) [1]. All these aspects can be explicitly tested also in a nuclear environment, using data from an increasing number of experiments that have performed very precise measurements of inclusive hadron production off nuclear targets. They comprise semi-inclusive measurements of hadron multiplicities by HERMES [6], as well as experiments in deuteron-gold (dAu) collisions at the BNL-RHIC [15–17]. Both processes show clear signals of a nontrivial nuclear dependence in the hadronization mechanism.

In addition to our primary goal, which is testing the factorization properties of nFFs in a consistent theoretical framework, we also aim to constrain them as precisely as possible from the different data sets currently available. This will allow one to compare our results for the nFFs with the different model estimates and mechanisms proposed to model hadronization in a nuclear medium [7,8]. Together with our analysis of vacuum FFs [1], the present work also serves as a baseline for ongoing studies of processes with detected hadrons in heavy-ion collisions performed at BNL-RHIC and at the CERN-LHC in the future. These projects are aimed at investigating the properties of hot and dense QCD matter, and require precise knowledge on hadronization under both normal and such extreme conditions [18].

The paper is organized as follows: in the next section, we very briefly summarize the pQCD framework for FFs and discuss how to extend it to nFFs, specifically for the processes on which we will base our analysis. We also review the different aspects of the data that suggest medium-induced effects in fragmentation processes. In Sec. III, we first show how the main features of the experimental results can be reproduced in a very basic scheme of medium modifications, associated with a simple parametrization of nFFs which can be motivated by intuitive arguments. Next, we present our results of a more refined determination of the medium modified fragmentation functions for pions at NLO accuracy. We briefly comment on different centrality classes in deuteron-gold collisions at RHIC. Finally, we extend our analysis to measurements of kaon production in a nuclear environment. We summarize our results in Sec. IV.

II. QCD FRAMEWORK FOR MEDIUM MODIFIED FRAGMENTATION FUNCTIONS

A. Basic properties of FFs

In the naive parton model, fragmentation functions $D_i^H(z)$ are simply taken as the probabilities for a final-state parton of a given flavor i to produce a specific hadron H, carrying a fraction z of its four-momentum. This intuitive picture can be consistently extended to the field-theoretical language of QCD by defining fragmentation functions in terms of bilocal operators in a certain factorization scheme [19]. The most common choice for the latter is the $\overline{\text{MS}}$ scheme, which we also adopt throughout this work. Along with analogous operator definitions for the parton distribution functions (PDFs), the factorization of short- and long-distance contributions to one-hadron inclusive cross sections is then precisely determined, and higher order QCD corrections can the be systematically taken into account.

While the nonperturbative but universal FFs (and PDFs) need to be extracted from data through global QCD analyses, both the relevant hard partonic scattering cross sections and the scale evolution of FFs (and PDFs) are calculable within pQCD. Corrections to this factorized framework emerge as inverse powers of the hard scale characterizing the one-hadron inclusive cross section, like the virtuality Q^2 of the exchanged virtual photon in e^+e^- annihilations or the transverse momentum p_T of the produced hadron in proton-proton collisions. Provided that Q^2 or p_T are large enough, these higher twist contributions can be safely neglected in phenomenological applications.

The scale dependence of the D_i^H is governed by a set of coupled renormalization group equations very similar to those for PDFs. They schematically read [20,21]:

$$\frac{d}{d\ln Q^2}\vec{D}^H(z,Q^2) = [\hat{P}^{(T)} \otimes \vec{D}^H](z,Q^2), \tag{1}$$

where

$$\vec{D}^{\,H} \equiv \begin{pmatrix} D_\Sigma^H \\ D_g^H \end{pmatrix}, \qquad D_\Sigma^H \equiv \sum_q (D_q^H + D_{\bar{q}}^H) \tag{2}$$

and

$$\hat{P}^{\,(T)} \equiv \begin{pmatrix} P_{qq}^{(T)} & 2n_f P_{gq}^{(T)} \\ \frac{1}{2n_f} P_{qg}^{(T)} & P_{gg}^{(T)} \end{pmatrix} \tag{3}$$

is the matrix of the singlet *timelike* evolution kernels. The symbol $\otimes$ denotes a standard convolution. The NLO splitting functions $P_{ij}^{(T)}$ have been computed in [20,21] or can be related to the corresponding spacelike kernels by proper analytic continuation [22]. Recently, the diagonal splitting functions $P_{qq}^{(T)}$ and $P_{gg}^{(T)}$ have been calculated up to next-to-next-to-leading order accuracy [23].

Apart from the requirement of a sufficiently large hard scale to suppress power corrections, the applicability of FFs is in practice further limited to the range of medium-to-large momentum fractions z [1–3]. While large perturbative contributions to the splitting kernels $P_{gq}^{(T)}$ and $P_{gg}^{(T)}$ at small z can be resummed to all orders, there is no systematic or unique way to include corrections related to the ignored mass of the produced hadron H. In any case, ''resummed'' or ''mass corrected'' FFs obtained in one process should not be used with fixed order expressions in other processes. However, it is a key point of global QCD analyses of FFs to combine diverse sets of data in their determination [1]. Only by consistently exploiting a large variety of one-hadron inclusive processes one can test the underlying assumption of factorization, implying that FFs are exactly the same no matter if the seed parton is excited from the vacuum like in e^+e^- annihilation or from a nucleon in the case of one-particle-inclusive processes in either lepton-nucleon or nucleon-nucleon collisions. To avoid problems at small z, we follow Ref. [1] and simply impose a cut $z > z_{\min} = 0.05(0.1)$ on all data with identified pions (kaons) used in our analysis of medium modified fragmentation functions.

B. Convolution approach for medium modified FFs

Assuming that hard collinear factorization for one-particle inclusive processes is realized also for collisions involving nuclei, one can define fragmentation functions $D_{i/A}^H(z)$ specific for nuclear environments characterized by their atomic number A. Like standard FFs, the medium modified $D_{i/A}^H(z)$ describe the hadronization of a parton i into a hadron H but now in the background of a nucleus A. Because of medium-induced final-state soft exchanges which happen after the hard partonic scattering process, the nonperturbative content of the $D_{i/A}^H(z)$ could differ significantly from the one known for vacuum fragmentation functions $D_i^H(z)$. A similar reasoning is applied with great phenomenological success in analyses of nPDFs that account for medium-induced effects in the initial state [11–13].

Provided that both FFs and nFFs have the same factorization properties and scale evolution equations, which are the crucial assumptions to be adopted and scrutinized in this analysis, we can use exactly the same theoretical expressions in computations of measured hadron yields for processes involving free or nuclear bounded nucleons, replacing only the PDFs and FFs by the corresponding nPDFs and nFFs in the latter case. The global analysis of the nFFs, that is the precise determination of the medium-induced modifications to FFs based on the presently available data, proceeds in close analogy to those for FFs. The stringent framework of pQCD and factorization does not require one to make any specific assumptions on the size and sign of nuclear modifications prior to the fit, and the results are entirely determined by data. Known nuclear effects on parton densities, as seen, e.g., in DIS off nuclei [9], are fully accounted for by choosing a recent set of nPDFs. The obtained sets of nFFs will allow us to test how well the underlying assumption of factorization works in practice and can be compared to the different ideas and mechanisms for medium modifications of quark and gluon FFs proposed in the literature [7,8]. We refer the reader to Ref. [1] for detailed expressions of the relevant cross sections and an outline of the numerical fitting procedure.

Rather than fitting from scratch the nFFs, which would take as many parameters as the standard or vacuum FFs, plus several more to represent their nuclear A dependence, we choose to relate the $D_{i/A}^H$ to the standard ones D_i^H at a given initial scale $Q_0 = 1$ GeV by a convolution approach:

$$D_{i/A}^H(z,Q_0^2) = \int_z^1 \frac{dy}{y} W_i^H(y,A,Q_0^2) D_i^H\left(\frac{z}{y},Q_0^2\right). \tag{4}$$

The weight function $W_i^H(y,A,Q_0^2)$ parametrizes all nuclear modifications and, at the same time, retains the information

already available on the vacuum FFs for $A = 1$. Here we take the NLO sets of DSS [1] as reference, which provide an excellent global description of hadron yields in e^+e^-, ep, and pp processes. We refrain from performing our analysis at leading order accuracy which, at best, can give a rough qualitative result. The LO FFs in Ref. [1] yield a significantly less favorable description of the data. Provided that the functional form for $W_i^H(y, A, Q_0^2)$ is flexible enough, one can accommodate the specific details of each individual measurement, and the nFFs can be extracted as precisely as possible from data. Notice that W_i^H depends only implicitly on Q_0 through the values obtained for the fitted parameters describing its functional form. The scale dependence of the nFFs in Eq. (4) is dictated by factorization and determined by the standard evolution equations for vacuum FFs discussed in Sec. II A. Even though the weight functions in principle inherit constraints from the standard set of sum rules that should be obeyed by fragmentation functions, the need to impose a cut $z > z_{\min}$ prevents them from being viable constraints in global analyses.

The impact of the weight function $W_i^H(y, A, Q_0^2)$ in Equation (4) on the resulting nFFs can be readily understood. A simple Dirac delta function $\delta(1 - y)$ as weight would imply no medium-induced effects in the hadronization process, while a shift in its argument, i.e., $\delta(1 - \epsilon - y)$, leads to a shift in the momentum fraction z as suggested, for instance, by many parton energy loss scenarios [7,8]. A more flexible weight function like

$$W_i^H(y, A, Q_0^2) = n_i y^{\alpha_i}(1 - y)^{\beta_i}, \tag{5}$$

can be used to parametrize effects not necessarily related to partonic mechanisms, such as hadron or prehadron attenuation or enhancement, with a great economy of parameters. As will be shown below, the A dependence of the weight function W_i^H can easily be included in its coefficients, e.g., n_i, α_i, and β_i in (5), by taking them as smooth functions of a nuclear property like its volume, radius, or mean density.

We note that convolutional integrals like in Eq. (4) are the most natural language for parton dynamics at LO and beyond, showing up ubiquitously in evolution equations, cross sections, etc. They can be most straightforwardly handled in Mellin moment space, which is also well suited for a numerically efficient global QCD analysis [24]. The convolution approach has been demonstrated to be effective and phenomenologically successful in the extraction of initial-state nuclear effects for PDFs at NLO accuracy in Ref. [11]. For consistency, we take these sets of nPDFs, in the following labeled as nDS, in all calculations of cross sections relevant for our global analysis of nFFs.

C. Data sensitive to nFFs

The gross features of FFs are usually determined from very precise e^+e^- annihilation data, mainly taken by the CERN-LEP experiments. The lack of this source of information for medium modified fragmentation functions is evident and significantly complicates their analysis. All available probes require a careful deconvolution of nFFs from medium effects related to nPDFs, which can be done consistently in a global QCD analysis based on factorization.

One of the most interesting pieces of evidence on medium-induced effects in the hadronization process comes from semi-inclusive deep-inelastic scattering off nuclear targets. Such kinds of measurements have been performed since the late seventies by different collaborations [5] and in recent years have reached a level of precision and sophistication that allows for very detailed quantitative analyses. Specifically, the HERMES collaboration has performed a series of measurements on deuterium, helium, neon, krypton, and xenon targets, with identified charged and neutral pions, kaons, and (anti)protons in the final state [6]. The data are presented as distributions in the relevant kinematical variables, such as the hadron momentum fraction z and the photon virtuality Q^2, which are used to characterize fragmentation functions, as well as the virtual photon energy ν, that can be related to the nucleon momentum fraction x carried by initial-state parton. In addition, very precise experimental studies have been presented recently in terms of p_T^2, the transverse momentum squared of the observed hadron. Even though the full NLO framework for the p_T dependent hadron yields in SIDIS processes is available [25], we choose to work only with p_T integrated results for the time being. The dependence of the data on this variable is rather weak, and the p_T values accessible so far are at the limit of a perturbative treatment. The detailed kinematical dependence of the HERMES data [6], combined with the information for different final-state hadrons and target nuclei, puts very sharp constraints on the effective, medium modified fragmentation functions we wish to determine.

In order to minimize initial-state medium-induced effects, which in a factorized approach should be contained in the nPDFs, the data are presented as ratios of hadron multiplicities for heavy nuclei A and deuterium (d),

$$R_A^H(\nu, Q^2, z, p_T^2) = \frac{\left(\frac{N^H(\nu,Q^2,z,p_T^2)}{N^e(\nu,Q^2)}\right)_A}{\left(\frac{N^H(\nu,Q^2,z,p_T^2)}{N^e(\nu,Q^2)}\right)_d}. \tag{6}$$

$N^H(\nu, Q^2, z, p_T^2)$ denotes the number of hadrons of type H produced in SIDIS, and $N^e(\nu, Q^2)$ is the number of inclusive leptons in DIS. The cancellation of initial-state nuclear effects would be exact in a LO framework if medium-induced modifications to the PDFs could be represented by a single multiplicative factor irrespective of the parton flavor. Even though the different parton species are known to require different, nontrivial modifications [11], these differences get diluted even at NLO accuracy. As will be shown below, they cancel in the ratio (6) to a very good approximation.

The second crucial piece of evidence on medium-induced effects in the hadronization process comes from single-inclusive identified hadron yields obtained in dAu collisions at midrapidity by the RHIC experiments at BNL [15–17]. These measurements are often seen as ''control experiments'' associated with the program of colliding two heavy-ion beams at RHIC to explore the properties of nuclear matter under extreme conditions. However, in the face of the clear evidence of strong medium-induced effects in the fragmentation process deduced from the SIDIS data [6], the dAu data [15–17] also acquire a particular relevance for our analysis.

Nuclear effects on hadron production in dAu collisions are often quantified through comparison to the corresponding pp spectrum, scaled by the average nuclear overlap or geometry function $\mathcal{N}$. The so defined nuclear modification factor [15–17]

$$R^H_{\rm dAu} \equiv \frac{1}{\mathcal{N}} \frac{Ed^3\sigma^H/dp^3|_{\rm dAu}}{Ed^3\sigma^H/dp^3|_{pp}}, \tag{7}$$

reflects not only the medium-induced effects on the fragmentation process, but also on the PDFs and includes possible deviations due to isospin considerations. $\mathcal{N}$ counts the number of underlying inelastic nucleon-nucleon (binary) collisions and depends on Glauber model calculations [15–17]. Experimental results for nucleon modification factors and invariant cross sections are divided into different centrality classes or presented for the combined minimum bias sample.

Surprisingly, instead of the pronounced hadron attenuation seen in nuclear SIDIS data [6], i.e., $R^H_A < 1$, the nuclear modification factors in dAu collisions show a curious pattern enhancement and suppression depending on p_T [15–17]. The interpretation of these results is complicated by the large amount of contributing partonic subprocesses with either quark or gluon fragmentation into the observed hadron H. Their individual share to the hadron yield is strongly correlated with p_T as will be shown in some detail below.

Rather than using the invariant cross sections, whose theoretical estimates suffer from a sizable dependence on the choice of the factorization scale μ_f [26], we perform the global fit in terms of the ratio of the dAu minimum bias cross section to the corresponding invariant hadron yield in pp collisions,

$$R^H_\sigma(A, p_T) \equiv \frac{1}{2A} \frac{Ed^3\sigma^H/dp^3|_{dA}}{Ed^3\sigma^H/dp^3|_{pp}}, \tag{8}$$

normalized by the number of participating nucleons. The advantage of R^H_σ is that both numerator and denominator can be computed consistently within pQCD at NLO accuracy using current sets of PDFs [27], nPDFs [11], and FFs [1]. In addition, the dependence on μ_f as well as normalization errors associated with inaccuracies in determinations of the PDFs and FFs tend to cancel in the ratio (8). As compared to the related nuclear modification factor $R^H_{\rm dAu}$, the ratio R^H_σ is less sensitive to estimates based on model dependent calculations. It is worthwhile noticing that the DSS set of FFs [1] was obtained from a global analysis using the same pp collision data we use to define the ratios in Eq. (8).

The convoluted way in which the information on quark and gluon fragmentation is encoded in dAu hadron production data is not an obstacle in a factorized approach since we can explicitly compute the relevant cross sections in terms of nPDFs and nFFs, as we do for SIDIS. In our global analysis, both sets of data will be treated simultaneously at NLO accuracy, and the optimum set of quark and gluon nFFs will be extracted. In this way we can test whether the hadron attenuation found in SIDIS off nuclei can be matched with the complicated pattern of enhancement and suppression observed in dAu collisions.

The fact that SIDIS is strongly dominated by quark fragmentation suggests that quark nFFs will be suppressed. Likewise, from the known dominance of gluons in pp collisions at RHIC in the relevant low-to-medium p_T region [26], one expects that the main medium-induced effect for them would be an enhancement. In the following we describe the details of our global analysis of nFFs, present the obtained z and A dependence of quark and gluon nFFs for pions and kaons, and show that the above, naive expectations are qualitatively correct.

The obtained nFFs apply to the production of hadrons in processes where a nucleus collides with a lepton, a nucleon, or a very light nucleus like deuterium. For collisions between two heavy nuclei the distinctive properties of the created hot and dense matter presumably may emphasize very different effects in the hadronization which perhaps even break factorization. This is beyond the scope of this first analysis of nFFs and requires more detailed studies in the future.

III. RESULTS

A. Determination of the weight functions

In order to give a first impression of the main features of medium-induced effects in the hadronization process suggested by the SIDIS [6] and dAu [15–17] data, we start with an extremely simple assumption for the functional form of the weight functions $W^H_i(y, A, Q^2_0)$ in Eq. (4). This will also illustrate the use and convenience of the convolution approach outlined in Sec. II B.

As we have mentioned in Sec. II C, the HERMES SIDIS data show a z dependent hadron attenuation $R^H_A < 1$ that increases with A [6]. Since the R^H_A do not significantly depend on the different pion charges, $H = \{\pi^-, \pi^0, \pi^+\}$, it is natural to assume the same medium effect on the fragmentation probability for both quarks and antiquarks. The observed reduction is most economically implemented by a weight function

$$W_q^\pi(y, A, Q_0^2) = n_q \delta(1-y) + \epsilon_q \delta(1-\epsilon_q - y) \quad (9)$$

that depends only on two free parameters n_q and ϵ_q. The changes induced in the quark fragmentation functions by such a weight are readily interpreted as the superposition of two mechanisms. The first term in (9) leads to a z independent overall reduction of the nFFs relative to the vacuum FFs, with n_q decreasing from unity with nuclear size A. The second term in (9) takes care of any nontrivial z dependence in R^H in the most simple way by shifting the effective value of z probed in the nuclear medium by a small amount ϵ_q which grows from zero with A. Such a shift is also suggested by models based on parton energy *loss*.

For gluons, one could try a similar weight function, however, low p_T pion yields in dAu collisions [15–17], where gluons are known to dominate in pp processes [26], suggest that the main effect should be an effective enhancement of the fragmentation probability rather than a reduction. Therefore n_g is most likely to be different from n_q. Other than in SIDIS, dAu data provide only information on the z dependence in a convoluted way, i.e., integrated over a certain range in z. Because of this, and to a first approximation, we simply take $\epsilon_g = \epsilon_q$. By removing this constraint, we find neither a noticeable improvement in the quality of the fit, nor any significant changes in the shape of the obtained gluon nFF.

The nuclear A dependence of the coefficients $n_{q,g}$ and $\epsilon_{q,g}$ parametrizing the naive weight functions $W_{q,g}^\pi$ in Eq. (9) can be easily implemented by a simple ansatz

$$n_q = 1 + \gamma_{n_q} A^{2/3}, \quad n_g = 1 + \gamma_{n_g} A^{2/3}, \quad \epsilon_q = \epsilon_g = \gamma_\epsilon A^{2/3}. \quad (10)$$

Such an A dependence could be motivated by the way in which the volume of a disk with nuclear radius $r_A \simeq r_0 A^{1/3}$ scales with A. In total this results in only three free parameters, $\{\gamma_{n_q}, \gamma_{n_g}, \gamma_\epsilon\}$, to be determined by the global fit.

As we will demonstrate in detail below, this very simple minded parametrization (in the following labeled as nFF*) reproduces to a good approximation the normalization and general trend of pion yields in SIDIS off nuclei and in dAu collisions. For completeness, the obtained coefficients parametrizing the naive weight functions are summarized in Table I. The ansatz in Eqs. (9) and (10) is, however, not flexible enough to satisfactorily describe more detailed features of the data, for instance, regarding the x dependence of R_A^π in SIDIS or the p_T dependence of the dAu data over the entire range. This is also reflected in the total χ^2 (to be defined below) per degree of freedom (dof) of such a fit, which is close to 2.

These shortcomings suggest that we need to implement much more flexible weight functions to fully exploit the constraining power of the data. In principle, these weights W_i^H could represent underlying mechanisms whose consequences would be other than overall changes in normalization and shifts in momentum fraction z, but still preserving factorization. Specifically, we adopt the following ansatz for our global analysis of nFFs for pions and kaons in Eq. (4),

$$W_q^H(y, A, Q_0^2) = n_q y^{\alpha_q}(1-y)^{\beta_q} + n_q' \delta(1-\epsilon_q - y),$$
$$W_g^H(y, A, Q_0^2) = n_g y^{\alpha_g}(1-y)^{\beta_g} + n_g' \delta(1-\epsilon_g - y), \quad (11)$$

discriminating between quarks and gluons. With the currently available data, no significant improvement of the fit is found by introducing an additional weight function for antiquarks different from the one used for quarks. In addition, the sensitivity of the data on the precise z dependence of the medium modified gluon fragmentation is not sufficient to allow for independent shifts ϵ_q and ϵ_g for quarks and gluons, respectively. Like in our simple ansatz in Eq. (9), we set $\epsilon_q = \epsilon_g$ without disturbing the quality or results of the fit, but we allow for $n_q' \neq n_g'$. The parametrizations of the weight functions in Eq. (11) can be seen as a natural extension of Eq. (9), where the first term can now have a flexible z dependence, and free coefficients n_i' add extra flexibility to the second, energy loss term.

The nuclear dependence of the coefficients in (11) can be again implemented as a smooth function in A,

$$\xi = \lambda_\xi + \gamma_\xi A^{\delta_\xi}, \quad (12)$$

where $\xi = \{n_{q,g}, \alpha_{q,g}, \beta_{q,g}, n'_{q,g}, \epsilon_{q,g}\}$, and the λ_ξ, γ_ξ, and δ_ξ need to be determined by the fit. Allowing for a completely unconstrained A dependence in (12) would require too many parameters, which in turn would be only poorly constrained by data. Some further guidance is provided by the requirement that nuclear effects should vanish as $A \to 1$, and the nFFs should turn into the well-known vacuum FFs. Since it is not entirely clear yet that this limit is smooth for small $A \lesssim 4$, we do not impose the additional constraint that $W_{q,g}^H$ approaches a delta function $\delta(1-y)$ as $A \to 1$. Nevertheless, in most cases λ_ξ can be set to zero or unity without damaging the quality of the global fit, and the corresponding values of γ_ξ stay very close to zero as

TABLE I. Coefficients parametrizing the naive weight functions $W_{q,g}^\pi$ in Eq. (9) at the input scale $Q_0 = 1$ GeV for different nuclei A. The three fitted parameters in Eq. (10) are shown in the last line.

A	n_q	$\epsilon_q = \epsilon_g$	n_g
He	0.966	0.001	1.015
Ne	0.902	0.002	1.044
Kr	0.745	0.006	1.115
Xe	0.657	0.008	1.155
Au	0.550	0.010	1.203
	$\gamma_{n_q} = -0.0133$	$\gamma_\epsilon = 0.003$	$\gamma_{n_g} = 0.006$

required by a smooth limit if $A \to 1$. In addition, some coefficients show a clear preference for a nuclear size dependence close to $A^{2/3}$. The assumption of this simple geometrical behavior with one common exponent δ_ξ for all the coefficients in (12) does not change the quality of the fit. In total this leaves 14 free parameters to be determined by the fit.

B. NLO analysis of pion nFFs

The free parameters in Eqs. (11) and (12), as well as for the simplified fit presented in the previous subsection, are determined by a standard χ^2 minimization for N data points, where

$$\chi^2 = \sum_{i=1}^{N} \frac{(T_i - E_i)^2}{\delta E_i^2}. \tag{13}$$

E_i is the measured value of a given observable, δE_i the error associated with this measurement, and T_i denotes the corresponding theoretical estimate for a given set of parameters. As often, we take statistical and systematical errors in quadrature in δE_i. Since this is the first attempt of an extraction of nFFs from a global QCD analysis, we refrain from a more sophisticated treatment of experimental uncertainties. In any case, full information on error correlation matrices is not available for most of the data sets being analyzed here.

The results of a fit based on the ansatz for the weight functions $W^\pi_{q,g}$ presented in Eqs. (11) and (12) is summarized in Tables II and III. In Table II we collect the values of the coefficients parametrizing the weight functions $W^\pi_{q,g}$ in Eq. (11) for different nuclei and the fitted parameters λ_ξ, γ_ξ, and δ_ξ in Eq. (12). Table III shows the partial contributions to χ^2 for each set of data included in the fit. We obtain an overall $\chi^2 = 396.0$ for 381 data points included in the analysis with 14 free parameters, resulting in an excellent $\chi^2/\text{dof} = 1.08$. Recall that the parameters of the simplified, three parameter fit based on Eqs. (9) and (10), which yields $\chi^2/\text{dof} \simeq 2$, were already presented in Table I.

The obtained smooth A dependence of the coefficients parametrizing the weight functions $W^\pi_{q,g}$ in Eq. (11) is illustrated in Fig. 1. Although not explicitly enforced in Eq. (12), $n'_{q,g}$ approaches unity and both $n_{q,g}$ and $\epsilon'_{q,g}$ tend to zero as $A \to 1$, as required by the vanishing of nuclear effects in that limit. As expected from the qualitative discussion of the data in Sec. II C, the pattern of medium-induced modification is rather different for quarks and for gluons. Most importantly, the normalizations n'_q and n'_g of the Dirac delta term in the convolution weights (11) have opposite signs, leading to suppression for the quark and enhancement for the gluon nFFs with respect to the vacuum FFs. The first term on the right-hand side of Eq. (11) also shows an opposite trend for quarks and gluons but influences mainly the small z behavior of the resulting $D^\pi_{q/A}$ and $D^\pi_{g/A}$ which will be presented at the end of this subsection.

In Fig. 2, the measured multiplicity ratios R^π_A for charged and neutral pions [6] are shown as a function of z, x, and Q^2 for different target nuclei A. To demonstrate the significance of medium modifications in the hadronization process, the dashed lines correspond to calculations of R^π_A at NLO accuracy using nPDFs from nDS [11] but standard DSS fragmentation functions [1]. All computations of multiplicities on a deuterium target in the denomi-

TABLE III. Data sets included in the NLO global analysis of pion nFFs, the individual χ^2 values for each set, and the total χ^2 of the fit.

Experiment	A	H	Data type	Data points	χ^2
HERMES [6]	He, Ne, Kr, Xe	π^+	z	36	39.3
		π^-	z	36	23.0
		π^0	z	36	27.4
		π^+	x	36	69.4
		π^-	x	36	55.4
		π^0	x	36	49.7
		π^+	Q^2	32	21.0
		π^-	Q^2	32	27.1
		π^0	Q^2	32	34.7
PHENIX [15]	Au	π^0	p_T	22	13.7
STAR (prel.) [17]	Au	π^0	p_T	13	12.8
STAR [16]	Au	$\pi^\pm$	p_T	34	22.5
Total				381	396.0

TABLE II. Coefficients parametrizing the weight functions $W^\pi_{q,g}$ in Eq. (11) at the input scale $Q_0 = 1$ GeV for different nuclei A. The 14 fitted parameters λ_ξ, γ_ξ, and δ_ξ in Eq. (12) are given in the bottom half of the table.

A	n'_q	$\epsilon_q = \epsilon_g$	n_q	α_q	β_q	n'_g	n_g	α_g	β_g
He	0.949	0.002	0.024	24.18	26.80	1.042	−0.131	19.50	46.24
Ne	0.863	0.006	0.065	23.54	26.13	1.114	−0.351	19.21	41.78
Kr	0.668	0.015	0.157	22.10	24.62	1.276	−0.849	18.56	31.72
Xe	0.564	0.020	0.206	21.33	23.81	1.362	−1.115	18.21	26.33
Au	0.439	0.026	0.265	20.41	22.85	1.466	−1.433	17.79	19.90
λ_ξ	1	0	0	24.56	27.20	1	0	19.67	48.88
γ_ξ	−0.022	0.001	0.010	−0.161	−0.169	0.018	−0.056	−0.073	−1.126
δ_ξ	0.615	0.615	0.615	0.615	0.615	0.615	0.615	0.615	0.615

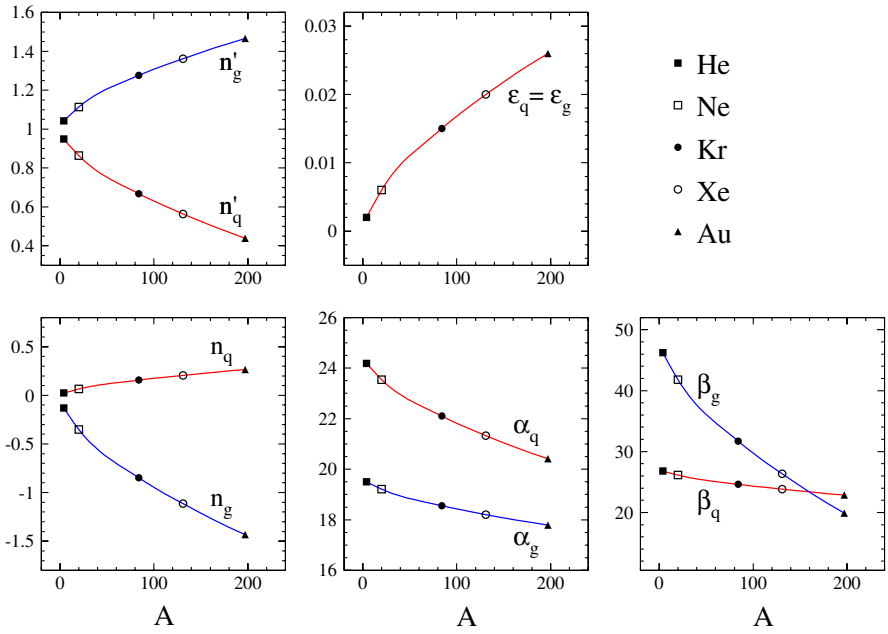

FIG. 1 (color online). A dependence of the coefficients parametrizing the weight functions $W^{\pi}_{q,g}$ in Eqs. (11) and (12).

nator of Eq. (6) are performed with Martin-Roberts-Stirling-Thorne PDFs [27] and DSS [1] FFs. As anticipated in Sec. II C, initial-state nuclear effects approximately cancel in R^{π}_{A}, and the results computed in this way are very close to unity for all kinematic distributions, in sharp contrast to data. Very similar results are obtained if other current sets of nPDFs [12,13] are used.

Notice that despite cancellations of the initial-state effects associated to the nPDFs, the measured medium-induced modifications of the pion multiplicities can be as large as a 50 percent effect for the heavier nuclei. They show a nontrivial z and x dependence, increase with the nuclear mass number A, and are most conspicuous for larger hadron energy fractions z and larger x, i.e., smaller ν. The dependence on Q^2, displayed in the bottom panel of Fig. 2, is comparatively flat but noticeable. Several models proposed to estimate medium-induced effects in the hadronization process reproduce some of the features of the data. However, the full kinematical dependence of $R^{H}_{A}(\nu, Q^2, z, p_T^2)$ is still a challenging issue; see Refs. [7,8] and references therein.

The results of the global analysis of nFFs based on the convolution approach are shown as dotted and solid lines for the naive three parameter and the refined ansatz for the weight functions $W^{\pi}_{q,g}$ introduced in Sec. III A, respectively. Both fits give a much superior description of the full kinematic dependence of the HERMES data than an approach which ignores final-state nuclear effects. Even the simple ansatz is doing surprisingly well in reproducing the general trend of the data, with some tensions in the x and z differential yields for larger nuclei. The latter are less significant for our more flexible parametrization. The trend of the data for small x, i.e., large ν, is of particular interest since one may expect that $R^{H}_{A} \longrightarrow 1$ as $\nu \longrightarrow \infty$, see, e.g., [8]. With presently available data it is, however, not possible to conclude if the disagreement between the fit and the data for $x \simeq 0.05$ ($\nu \approx 20$) for the largest nuclei gives a first hint at possible factorization breaking effects. The occurrence of a discrepancy in one corner of the kinematic region explored by a fit most often only points towards lack of flexibility in the assumed functional form. More precise data with an extended coverage towards larger ν are needed for further studies. It is interesting to notice that there seems to be no visible conflict between the standard Q^2 dependence assumed for the nFFs in our fit and the data. In this respect, there have been many interesting suggestions and model dependent calculations at the LO level, motivating the use of medium modified evolution equations; see [14] and references therein. However, in the range of Q^2 covered by present SIDIS data, there is no evidence for a significant departure from standard timelike evolution equations and kernels in Eqs. (1) and (3), respectively.

In Figs. 3–5 we show both the invariant dAu cross sections for neutral and charged pion production at RHIC as a function of p_T, and, in the lower panels, the ratios R^{h}_{σ} to the pp yields, defined in Eq. (8). Because of the steep fall of the cross sections with p_T over several orders of magnitude in the range shown in Figs. 3–5, it is hard to see any differences between the data and the NLO calculations based on standard or medium modified FFs. They become clearly visible, however, in terms of the ratios R^{h}_{σ} and can be as large as about 20%.

At variance with R^{π}_{A} in SIDIS, where initial-state medium effects, and hence the differences associated to the choice of nPDFs, cancel to a large extent, they may remain

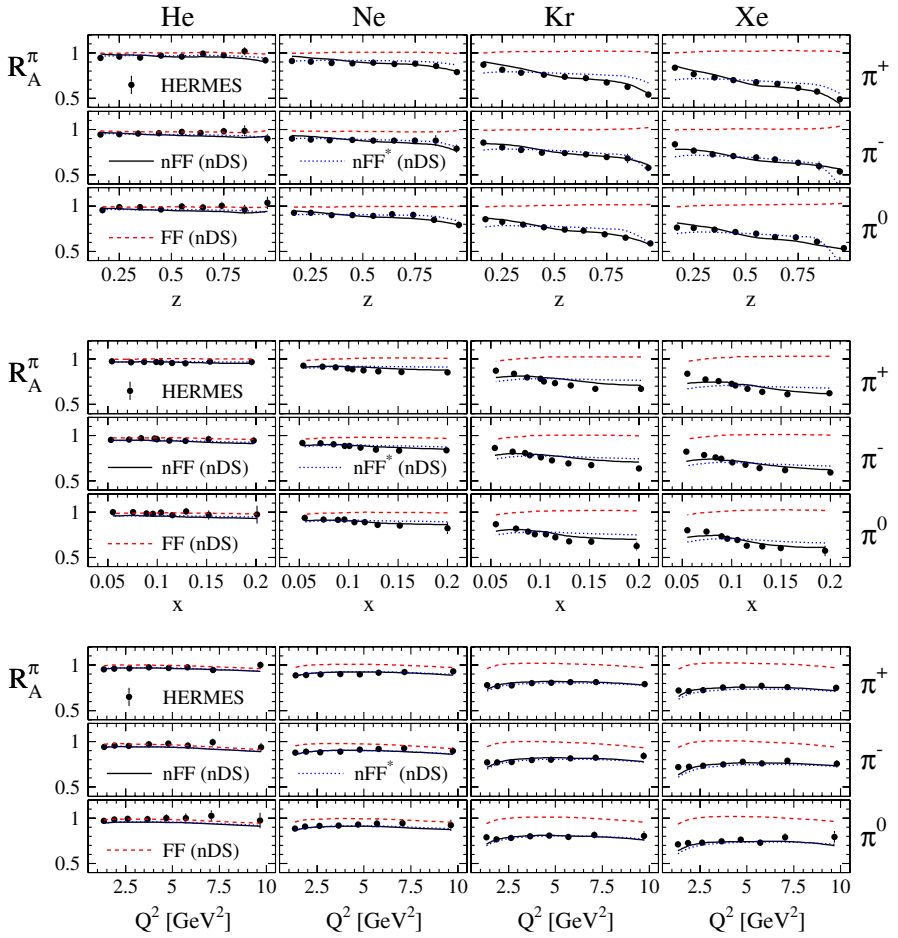

FIG. 2 (color online). R_A^π in SIDIS for different nuclei in bins of z (upper panel), x (middle panel), and Q^2 (bottom panel) as measured by HERMES [6]. The solid lines correspond to the results of our optimum fit for nFFs using the nDS medium modified parton densities [11]. The corresponding fit based on the simple nFF* ansatz in Eq. (9) is shown as dotted lines. The dashed lines are estimates assuming the nDS medium modified PDFs but standard DSS vacuum FFs [1].

significant for dAu data. Thus, estimates of the medium-induced modifications for fragmentation functions could in principle depend on the choice of nPDFs. To estimate their impact on the dAu cross sections and on the ratios R_σ^h, we use two different sets of nPDFs, nDS [11], and Eskola-Paukkunen-Salgado (EPS) [13], along with the well-known standard FFs of DSS for our calculations shown in Figs. 3–5. As can be seen, both results do not differ too much and fall short of describing the data satisfactorily, leaving room for improvement due to medium-induced effects in the hadronization process. The EPS set reproduces the trend of the data better than nDS, in particular, for neutral pions shown in Figs. 3 and 4, which extend to somewhat larger values of p_T than the charged pion data in Fig. 5. Notice, however, that the dAu data were included in the EPS analysis of nPDFs, but assuming nuclear effects in the hadronization process to be negligible [13]. Although the modification introduced in the EPS nPDFs helps to describe the dAu data better [13], neglecting final-state nuclear effects is clearly not advisable in view of their significant impact on R_A^π in SIDIS demonstrated in Fig. 2.

The results of our global fit of nFFs are shown in Figs. 3–5 as solid and dotted lines, corresponding to our optimum and simplified ansatz for the weight function $W_{q,g}^\pi$ introduced in Sec. III A, respectively. Here, the naive three parameter ansatz for $W_{q,g}^\pi$ fails to reproduce the p_T dependence of the dAu data, and the greater flexibility of Eqs. (11) and (12) is clearly needed and leads to a significant improvement of the fit. The simultaneous description of SIDIS and dAu data requires to have the correct balance between quark and gluon contributions in the fragmentation process, which is strongly p_T and, hence, z dependent.

An important difference between SIDIS and dAu data is that in the latter case the cross sections sample contributions from a wide range in z. Consequently, the deconvolution of the medium-induced effects is less transparent. In order to provide a better insight into the sensitivity of the RHIC measurements to the fragmentation process, we show in Fig. 6(a) the mean value of the hadron's fractional momentum z probed in pp and dAu collisions as a function of p_T. There are several ways to estimate an average $\langle z \rangle$. We define it in the standard way by evaluating the con-

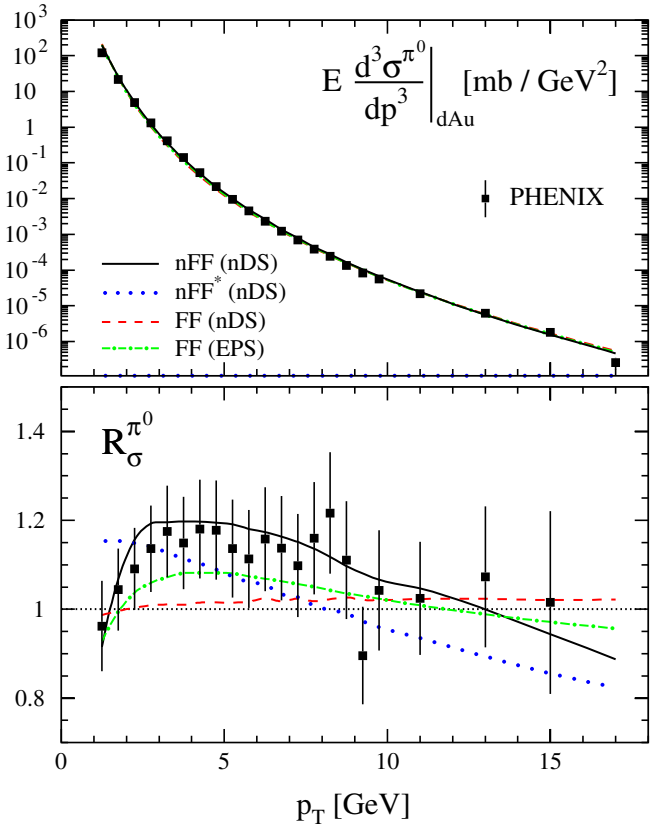

FIG. 3 (color online). Upper panel: comparison of the PHENIX data for neutral pion production in dAu collisions at midrapidity [15] with NLO estimates obtained with various combinations of nPDFs, FFs, and nFFs. The solid and dotted line correspond to the results of our optimum and simple three parameter fits for nFFs, respectively, using the nDS nPDFs [11]. Results based on standard DSS FFs [1] are shown as dashed and dot-dashed lines for nDS [11] and EPS [13] nPDFs, respectively. Lower panel: same as above but now for the ratio R_σ^π defined in Eq. (8).

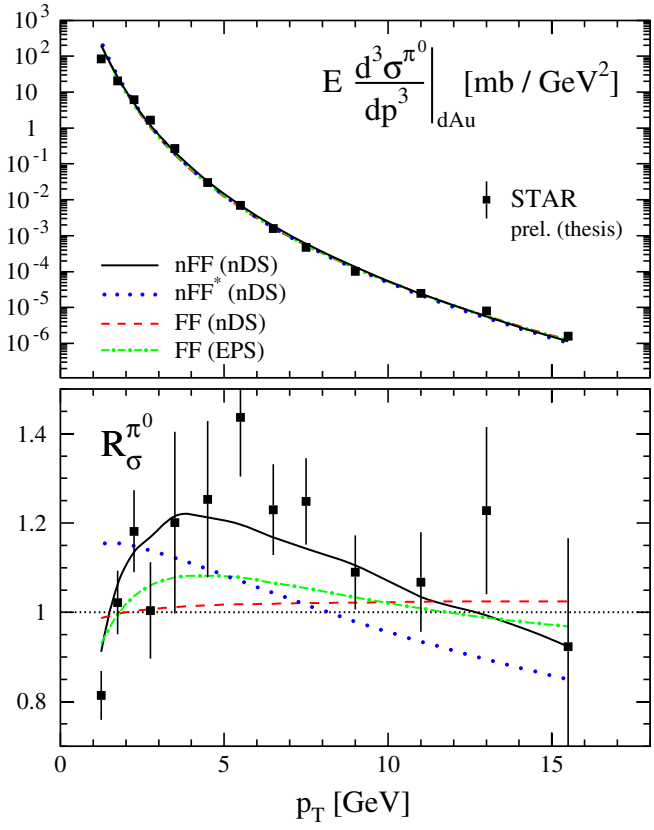

FIG. 4 (color online). The same as in Fig. 3 but now for neutral pion data obtained by STAR [17].

volutions in the factorized expression for the p_T dependent cross section [26] with an extra factor of z in the integrand, divided by the cross section itself [28], i.e., schematically we use

$$\langle z \rangle \equiv \frac{\int dz z \frac{d\sigma^H}{dz dp_T}}{\int dz \frac{d\sigma^H}{dz dp_T}}. \tag{14}$$

Here, $d\sigma^H/dzdp_T$ contains the appropriate convolutions of the parton densities and fragmentation functions with the partonic hard scattering cross sections.

Panel (b) of Fig. 6 shows the individual $\langle z \rangle$ for quark and gluon fragmentation processes, simply referring to the contributions in the dAu cross section proportional to either $D^\pi_{q/\mathrm{Au}}$ or $D^\pi_{g/\mathrm{Au}}$. Beyond the LO, this separation involves some arbitrariness and depends on the choice of the factorization scheme. In addition, primary partons created in the hard scattering may radiate off secondary partons of a different species which in turn fragment into the observed hadron. Figure 6(c) shows histograms of the z distribution for three representative values of p_T. In panel (d), we present the relative contributions of quark and gluon fragmentation processes to the π^0 production cross section in pp and dAu collisions.

As can be seen in Fig. 6, RHIC pp and dAu data are mainly sensitive to fairly large values of the momentum fraction taken by the hadron H, with $\langle z \rangle$ slightly increasing with p_T. However, as panel (c) shows, the cross section samples contributions over a broad range in z, starting at about $z \simeq 0.2$. Notice that below about $p_T = 1.5$ GeV, the tail in the z distribution becomes sensitive to values $z \lesssim 0.1$, where the concept of fragmentation functions breaks down due to finite hadron mass effects and the singular behavior of the timelike evolution kernels. It is also worthwhile mentioning that the values of z to which the cross sections are most sensitive to, i.e., $\langle z \rangle$, depend, of course, on the actual shape of the FFs and nFFs assumed in the analysis of pp and dAu collision data, respectively. Since we anticipate sizable differences between them, the ratios R_σ^H defined in Eq. (8) actually sample the nuclear and the vacuum fragmentation functions at slightly different values of z, cf. Fig. 6(a). This can have quite some effect on the ratios R_σ^H in regions where the fragmentation functions vary rapidly with z.

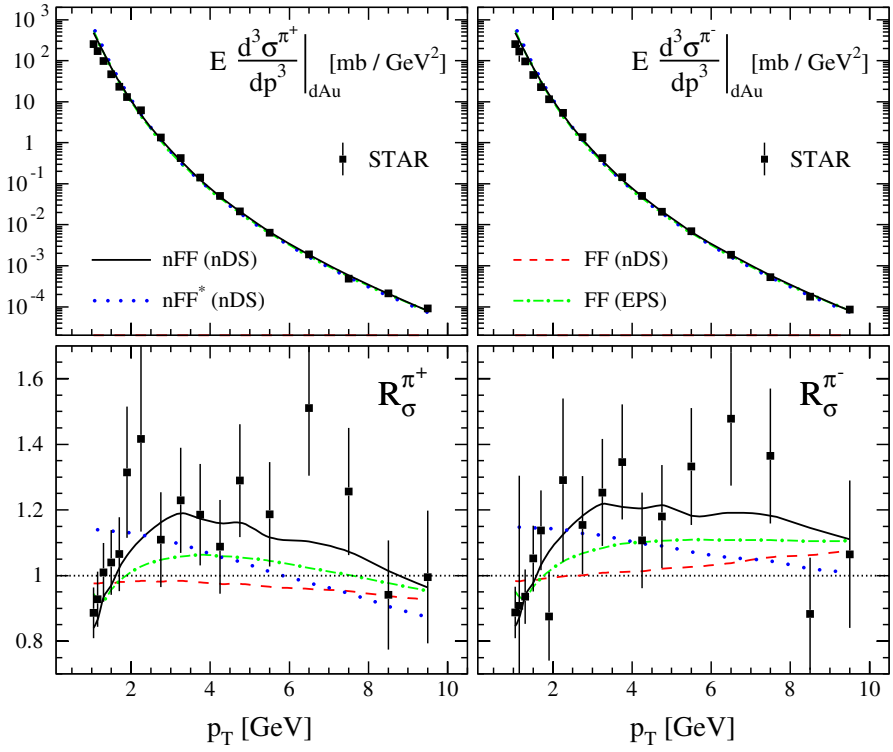

FIG. 5 (color online). The same as in Figs. 3 and 4 but now for charged pion data from STAR [16].

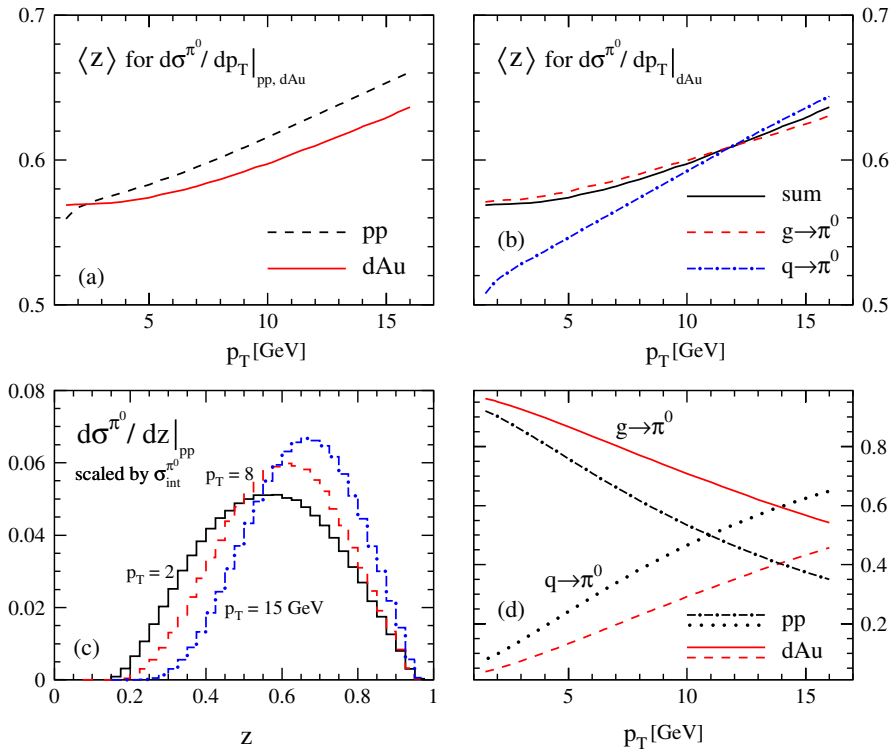

FIG. 6 (color online). (a) The mean value of z probed in pp and dAu collisions as a function of p_T. (b) The mean value of z in dAu collisions for both quark and gluon contributions. (c) Histograms of the z distribution for three representative p_T values. (d) The relative contributions of quark and gluon fragmentation processes to the π^0 production cross section in pp and dAu collisions.

Figure 6(d) demonstrates that for pp collisions gluon fragmentation is clearly the dominant production mechanism at low values of p_T. Quark fragmentation contributions increase with p_T, and cross the level of 50% at $p_T \simeq 10$ GeV. Again, the relative balance between quark and gluon contributions in dAu collisions will depend on the extracted medium-induced modifications. In our analysis, pion production is dominantly driven by gluon fragmentation up to the highest values of p_T, about 15 GeV, currently accessible in experiment. As we shall see below, this is due to the nuclear suppression of $D^H_{q/A}$ on the one hand, and enhancement of $D^H_{g/A}$ on the other hand.

The resulting modified fragmentation functions and the corresponding ratios to the standard DSS FFs,

$$R^H_q \equiv \frac{D^H_{q/A}(z, Q^2)}{D^H_q(z, Q^2)}, \qquad R^H_g \equiv \frac{D^H_{g/A}(z, Q^2)}{D^H_g(z, Q^2)}, \tag{15}$$

can be found in Fig. 7 at $Q^2 = 10$ GeV^2 for various nuclei. As expected from the qualitative discussion of the data in Sec. II C, the pattern of medium-induced modifications is rather different for quarks and for gluons. The dominant role of quark fragmentation in SIDIS leads to a suppression, i.e., $R^\pi_q < 1$, increasing with nuclear size A as dictated by the pattern of hadron attenuation found experimentally; see Fig. 2. The enhancement of hadrons observed in dAu collisions for $p_T \lesssim 10$ GeV, see Figs. 3–5, along with the dominant role of gluon fragmentation at low values of p_T explains that $R^\pi_g > 1$ for $z \gtrsim 0.2$. Below $z \simeq 0.2$, where all the data we analyze have very little or no constraining power, both quark and gluon nFFs drop rapidly. For the time being, the behavior in this region could easily be an artifact of the currently assumed functional form for the weights $W^H_{q,g}$ in Eq. (11).

We note that for $z \gtrsim 0.4$ the bulk of the medium-induced effects for both quarks and gluons can be accommodated by the second term in $W^H_{q,g}$ proportional to a Dirac delta function, which normalization coefficients n'_q and n'_g have to have opposite signs, reflecting suppression and enhancement, respectively. The other term in $W^H_{q,g}$ introduces only a small correction in this region, but becomes dominant if $z \lesssim 0.4$, especially for $D^H_{g/A}$.

We wish to stress, that even with the limited amount of data available at present, the successfully performed global analysis of nFFs provides a first nontrivial indication that the assumed factorization of long- and short-distance physics works amazingly well also for SIDIS off nuclei and dAu collisions at RHIC. The found suppression $R^\pi_q < 1$, as imposed by SIDIS data, is fully compatible with the complicated pattern of enhancement and attenuation of hadron yields in dAu collisions at RHIC. The non-negligible role of quark fragmentation in dAu collisions at moderate and large values of p_T, along with the larger nuclear effects for $D^H_{q/A}$ than for $D^H_{g/A}$ at large values of z, explains that $R^\pi_\sigma < 1$ for $p_T \gtrsim 10$ GeV. In addition, even though SIDIS data

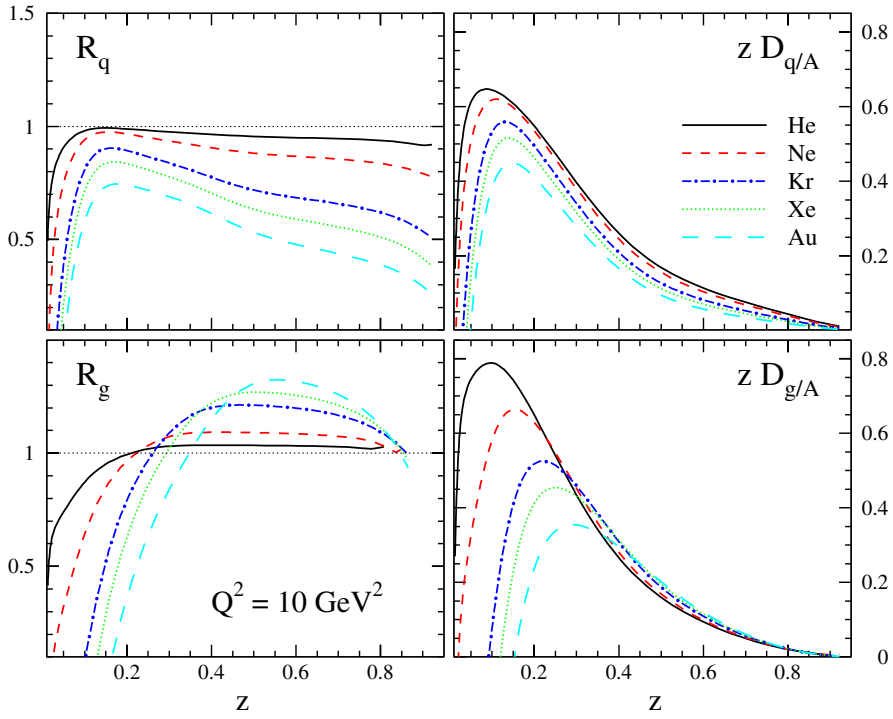

FIG. 7 (color online). The resulting medium modified NLO fragmentation functions for quarks and gluons into neutral pions at $Q^2 = 10$ GeV^2 for various different nuclei (right panels). The left panels show the corresponding ratios $R^\pi_{q,g}$ to the standard DSS FFs as defined in Eq. (15).

are dominantly sensitive to quark fragmentation, the observed nontrivial Q^2 and x dependence of the SIDIS multiplicity ratios shown in Fig. 2, depends on the medium-induced modifications of the gluon fragmentation function, which in turn is mainly, but not exclusively, constrained, by dAu data. At the level of the precision of our fit, the gluon nFF contributes noticeably to SIDIS through both the NLO corrections to the hard scattering process and the scale evolution. For instance, using the standard vacuum gluon FFs of DSS along with our obtained quark nFFs to compute R_A^π in Fig. 2, the results would differ by up to 10% from our best fit. The relevance of the gluon nFF in describing the SIDIS results also helps to pin down its A dependence. The correlation of the x dependence of SIDIS multiplicity rates with the z dependence of the fragmentation functions is induced by the NLO hard scattering coefficient functions which depend in a nontrivial way on both x and z; see, e.g., Ref. [29].

C. Dependence on different centrality classes

All the data on hadron yields in dAu collisions we have discussed and analyzed so far correspond to minimum bias events. Experiments also present their results divided into different centrality classes depending on how central or how peripheral the collision is in impact parameter space. In that respect, the nFFs obtained in our global analysis correspond to some sort of average of the medium-induced effects seen for the different degrees of geometrical overlap between the deuteron and the gold nuclei. One could expect that this average underestimates the medium-induced effects when the collisions are more central and overestimates them for the more peripheral ones.

To estimate the possible impact of different centrality classes on the extraction of nFFs, we scale our results obtained for the minimum bias cross sections shown in Figs. 3–5, by the average ratio between the measured cross section for a given centrality class (cc) and the minimum bias (mb) sample, i.e.,

$$\mathcal{C} \equiv \left\langle \frac{Ed^3\sigma^{\pi^0}/dp^3|^{\rm cc}_{\rm dAu}}{Ed^3\sigma^{\pi^0}/dp^3|^{\rm mb}_{\rm dAu}} \right\rangle_{\rm cc}. \tag{16}$$

The ratio (16) is a simple estimate of the fraction of events selected by a given centrality cut.

As a representative example, we show in Fig. 8 the comparison between the PHENIX data for four different centrality classes [15] and the corresponding minimum bias cross section computed with our nFFs and rescaled by $\mathcal{C}$. As expected, our nFFs slightly overestimate the data for the most peripheral events denoted by 40%–60% and 60%–88%. The agreement with the more central events is, however, very good, and we do not find the expected underestimate of nuclear effects. As for the minimum bias cross sections shown in Figs. 3–5, estimates obtained with standard vacuum FFs do not reproduce the trend of the data very well, except for the most peripheral events.

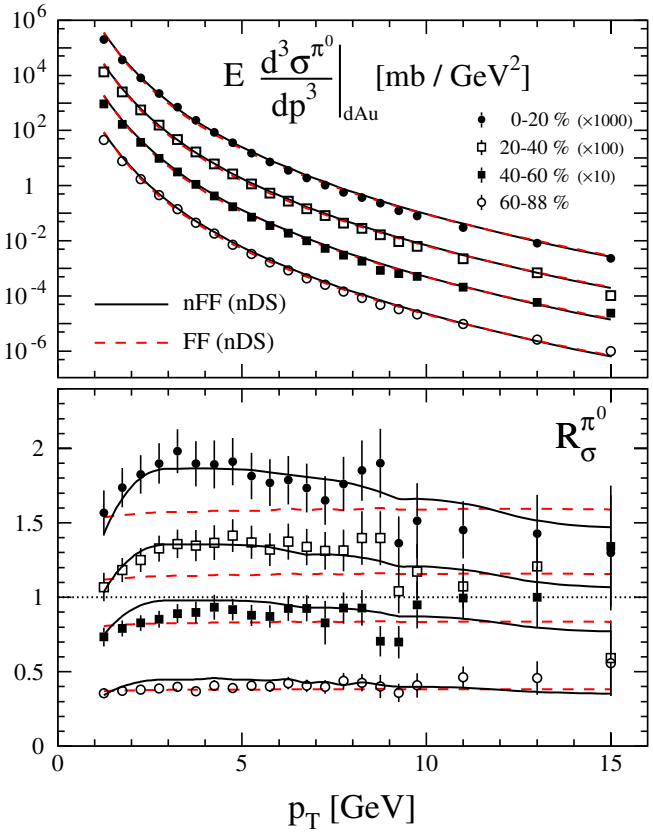

FIG. 8 (color online). As in Fig. 3 but now separated into different centrality classes ranging from the most central one, 0%–20%, to the most peripheral one, 60%–88%. The theoretical estimates obtained for minimum bias events are rescaled by the ratio $\mathcal{C}$ defined in Eq. (16) to account for the different centrality classes.

Results for pion yields in different centrality classes obtained by the STAR experiment are very similar to those presented in Fig. 8 and hence not shown. For completeness, Fig. 9 gives a comparison similar to those presented in the lower panel of Fig. 8 but now in terms of the nuclear modification factors.

D. NLO analysis of kaon nFFs

Even though the available experimental information on kaon production in a nuclear environment is much more limited than in the case of pions, it is interesting to study to what extent the pattern of nuclear modifications found for pions is similar to those for kaons. It should be noted that the standard kaon FFs, which will provide the baseline to analyze medium-induced effects, still suffer from sizable uncertainties [1].

In a scenario where the medium-induced modifications to the hadronization process are dominated by partonic mechanisms, and to a first approximation in a convolutional approach, one expects a very similar pattern of medium modifications for pions and for kaons. If interactions of the produced hadron or intermediate prehadrons

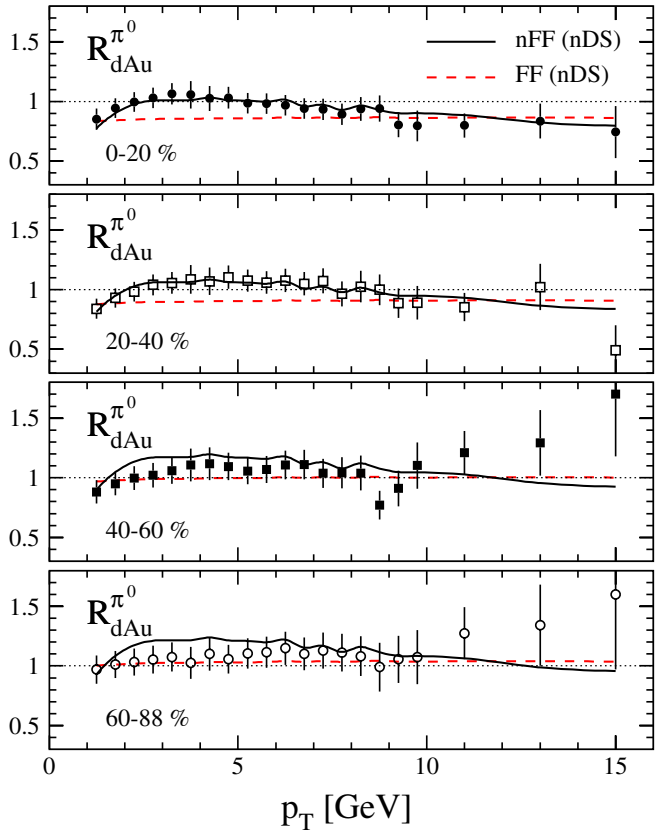

FIG. 9 (color online). As in the lower panel of Fig. 8 but now in terms of the experimentally determined nuclear modification factors $R^{\pi^0}_{\rm dAu}$ [15].

with the nuclear environment are important, medium-induced effects in the production of pions and kaons can be significantly different.

Because of the relative scarcity of data with identified kaons, especially in the case of dAu collisions where most of the data are taken at p_T values below the reach of perturbative QCD methods, we cannot proceed with our global analysis as we did pions. The coefficients of a completely flexible parametrization for the weights $W^K_{q,g}$ like in Eq. (11) would not be well constrained by the data. Therefore, our strategy is as follows: we start by imposing a more constrained ansatz for the weights $W^K_{q,g}$ where we assume some of the features of the medium-induced effects found for the pion nFFs. More specifically, we keep the same functional form for the weights as in Eq. (11), with the same nuclear A dependence as in Eq. (12). We also take over the simplifying assumption $\epsilon_q = \epsilon_g$, which we have chosen for pion nFFs in Secs. III A and III B after checking that more flexible options did not lead to a significant improvement of the quality of the fit. In addition, we try to set the exponents δ_ξ governing the A dependence in Eq. (12) to the values preferred by the pion data.

Next, we can assess how much variation of the other parameters relative to the results for the pion nFFs listed in Table II is required to reproduce the main features of the kaon data. We find that allowing for an up to 20% variation yields a more than reasonable agreement with all available data sets, with most of the parameters staying within a 10% variation of their counterparts describing the pion nFFs. In Table IV we list the values of the coefficients parametrizing the weight functions $W^K_{q,g}$ in Eq. (11) for different nuclei and the 13 fitted parameters λ_ξ and γ_ξ in Eq. (12); the δ_ξ are fixed to the values given in Table II.

The overall quality of the fit is summarized in Table V. The total χ^2 of the fit is 447.1 for 218 data points included in the global analysis, resulting in $\chi^2/{\rm dof} = 2.2$. Also given are the individual contributions to χ^2 for each set of data included in the fit. Even though the quality of the fit is not as good as in the case of pions, it reproduces the data well within their uncertainties and suggests a close similarity between the medium-induced modifications for pion and kaon fragmentation functions. As it could be expected, the most significant variations are found in the parameters related to the gluon fragmentation $D^K_{g/A}$, which are only poorly constrained by the scarce dAu data. Note that the largest individual contribution to χ^2 stems from the SIDIS data with identified K^- where already the vacuum FFs show some tension with the experimental results [1].

In Fig. 10 we compare the result of our fit with the measured SIDIS multiplicity ratios R^K_A for charged kaons as a function of z, x, and Q^2 for different target nuclei A. As can be seen, the agreement with the K^+ data is reasonably good with some problems in reproducing the x distributions for heavier nuclei. Discrepancies are somewhat larger for K^- data as we have already mentioned. For compari-

TABLE IV. Coefficients parametrizing the weight functions $W^K_{q,g}$ in Eq. (11) at the input scale $Q_0 = 1$ GeV for different nuclei A. The 13 fitted parameters λ_ξ and γ_ξ are given in the bottom half of the table. Note that the ϵ_ξ are chosen as in Table II.

A	n'_q	ϵ	n_q	α_q	β_q	n'_g	n_g	α_g	β_g
He	0.957	0.003	0.024	27.95	30.16	1.038	−0.107	17.75	39.37
Ne	0.884	0.007	0.065	27.37	29.55	1.103	−0.288	17.40	35.33
Kr	0.719	0.017	0.156	26.08	28.17	1.248	−0.695	16.60	26.22
Ze	0.630	0.022	0.205	25.38	27.43	1.326	−0.913	16.17	21.34
Au	0.525	0.028	0.264	24.55	26.55	1.419	−1.174	15.67	15.52
λ_ξ	1	0	0	28.29	30.52	1	0	17.96	41.76
γ_ξ	−0.0185	0.0011	0.0102	−0.1451	−0.1543	0.0163	−0.0456	−0.089	−1.020

TABLE V. Data sets included in the NLO global analysis of kaon nFFs, the individual χ^2 values for each set, and the total χ^2 of the fit.

Experiment	A	H	Data type	Data points	χ^2
HERMES [6]	He, Ne, Kr, Xe	K^+	z	36	61.3
		K^-	z	36	91.7
		K^+	x	36	67.2
		K^-	x	36	128.5
		K^+	Q^2	32	38.4
		K^-	Q^2	32	50.0
STAR [16]	Au	K^+	p_T	5	5.4
	Au	K^-	p_T	5	4.6
Total				218	447.1

son, we show again the results of a theoretical calculation based on standard vacuum FFs (dashed lines). As for the pion multiplicity ratios shown in Fig. 2, not even the trend of the data can be reproduced by ignoring medium-induced modifications to the hadronization process. Finally, Fig. 11 shows both the invariant dAu cross section for charged kaon production as a function of p_T, and, in the lower panels, the ratios R_σ^K to the corresponding pp yields. One should notice the limited range in p_T covered by the presently available data which is certainly at the borderline where pQCD is applicable. Nevertheless, our fit describes the data well except for the lowest bin in p_T.

The availability of both more precise kaon data and more accurate sets of vacuum FFs in the future, will help to further investigate the interesting and nontrivial close relation between the nuclear modifications for pion and kaon fragmentation functions found in our analysis.

IV. SUMMARY AND CONCLUSIONS

We have investigated the possibility of using a fully factorized approach at NLO accuracy of pQCD, similar to those established for analyses of standard FFs and PDFs, to describe medium-induced effects in the hadronization process.

To this end, we have explored the concept of modified fragmentation functions which effectively accounts for all the distortions in the production of hadrons caused by the nuclear environment. These novel distributions, which we denote as nFFs, are completely analogous to nuclear PDFs, and, combined with them, allow one to treat a large class of hard reactions where a nucleus collides with a lepton, a nucleon, or a very light nucleus like a deuteron in a consistent pQCD framework.

We have performed combined NLO fits to the available pion and kaon production data in SIDIS and in dAu collisions to reveal the nonperturbative features of the nFFs, exploiting the well-established potential of pQCD to describe hard scattering processes and the wealth of informa-

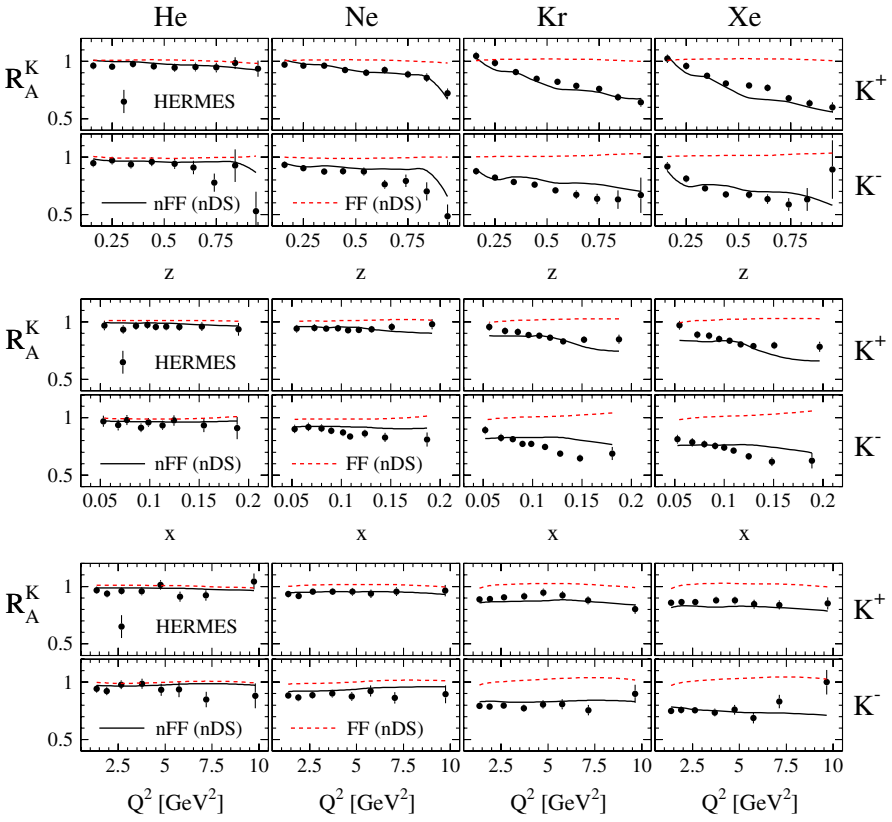

FIG. 10 (color online). As in Fig. 2 but now for identified $K^\pm$.

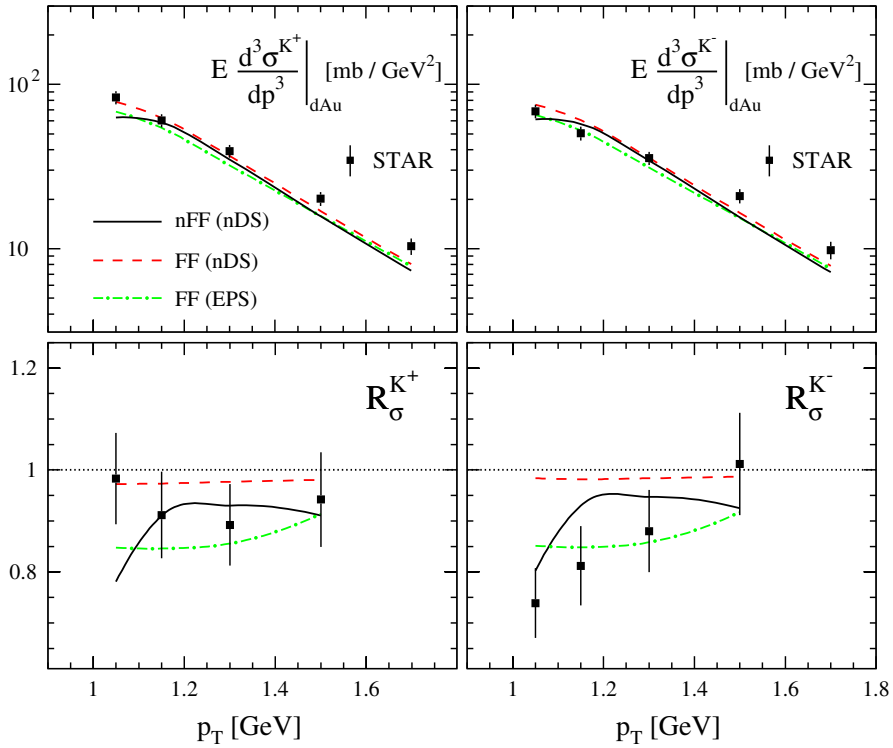

FIG. 11 (color online). As in Fig. 5 but now for charged kaon production.

tion compiled in PDFs and nPDFs over the past years. We choose to relate the nFFs to the well-known standard FFs in a convolutional approach with a great economy of free fit parameters, including a smooth dependence on the nuclear size A.

The obtained parametrizations of nFFs for pions and kaons [30] rather accurately reproduce the data and their nuclear A dependence. Our results provide support to the idea that conventional factorization of short and long-distance physics effects works to a good approximation also in the nuclear environments studied in our analyses. The found pattern of medium-induced modification is rather different for fragmenting quarks and gluons, where we find suppression and enhancement, respectively, compared to the vacuum fragmentation functions. Since our nFFs parametrize the available data without resorting to a certain model or underlying mechanism for the observed medium modifications, they may help to further our understanding on hadronization in a nuclear environment. Predictions based on the observed pattern for quark and gluon nFFs can be tested by upcoming data from JLab, BNL-RHIC, and CERN-LHC, and perhaps in the future at an electron-ion collider like the EIC project. This will help to understand the limits of the factorized approach which is expected to be only an approximation and may receive corrections beyond the leading twist level or beyond a pQCD approach.

ACKNOWLEDGMENTS

We warmly acknowledge Elke Aschenauer and Abhay Deshpande for help with the HERMES and RHIC data, respectively, and Daniel de Florian for helpful discussions. This work was partially supported by CONICET, ANPCyT, UBACyT, BMBF, and the Helmholtz Foundation.

[1] D. de Florian, R. Sassot, and M. Stratmann, Phys. Rev. D **75**, 114010 (2007); **76**, 074033 (2007).
[2] M. Hirai, S. Kumano, T. H. Nagai, and K. Sudoh, Phys. Rev. D **75**, 094009 (2007).
[3] S. Albino, B. A. Kniehl, and G. Kramer, Nucl. Phys. **B803**, 42 (2008).
[4] See, e.g., J. C. Collins, D. E. Soper, and G. Sterman, Perturbative QCD, edited by A. H. Mueller, Adv. Ser. Dir. High Energy Phys. 5, 1 (1988), and references therein.
[5] L. S. Osborne *et al.*, Phys. Rev. Lett. **40**, 1624 (1978); J. Ashman *et al.* (European Muon Collaboration), Z. Phys. C **52**, 1 (1991); M. R. Adams *et al.* (E665 Collaboration),

Phys. Rev. D **50**, 1836 (1994).
[6] A. Airapetian *et al.* (HERMES Collaboration), Nucl. Phys. **B780**, 1 (2007); Phys. Lett. B **684**, 114 (2010).
[7] F. Arleo, Eur. Phys. J. C **61**, 603 (2009).
[8] A. Accardi, F. Arleo, W. K. Brooks, D. D'Enterria, and V. Muccifora, Riv. Nuovo Cimento Soc. Ital. Fis. **032**, 439 (2010).
[9] P. Amaudruz *et al.* (New Muon Collaboration), Nucl. Phys. **B441**, 3 (1995); M. Arneodo *et al.* (New Muon Collaboration), Nucl. Phys. **B441**, 12 (1995); **B481**, 3 (1996); **B481**, 23 (1996).
[10] D. M. Alde *et al.*, Phys. Rev. Lett. **64**, 2479 (1990); M. A. Vasilev *et al.* (FNAL E866 Collaboration and NuSea Collaboration), Phys. Rev. Lett. **83**, 2304 (1999).
[11] D. de Florian and R. Sassot, Phys. Rev. D **69**, 074028 (2004).
[12] M. Hirai, S. Kumano, and T. H. Nagai, Phys. Rev. C **76**, 065207 (2007).
[13] K. J. Eskola, H. Paukkunen, and C. A. Salgado, J. High Energy Phys. 04 (2009) 065.
[14] X. F. Guo and X. N. Wang, Phys. Rev. Lett. **85**, 3591 (2000); A. Majumder, E. Wang, and X. N. Wang, Phys. Rev. C **73**, 044901 (2006); N. Armesto, L. Cunqueiro, C. A. Salgado, and W. C. Xiang, J. High Energy Phys. 02 (2008) 048; S. Albino, B. A. Kniehl, and R. Perez-Ramos, Nucl. Phys. **B819**, 306 (2009).
[15] S. S. Adler *et al.* (PHENIX Collaboration), Phys. Rev. Lett. **98**, 172302 (2007).
[16] J. Adams *et al.* (STAR Collaboration), Phys. Lett. B **616**, 8 (2005); **637**, 161 (2006).
[17] O. Grebenyuk, Ph.D. thesis, University of Utrecht [arXiv:0909.3006].
[18] See, e.g., N. Armesto, arXiv:0903.1330.
[19] J. C. Collins and D. E. Soper, Nucl. Phys. **B193**, 381 (1981); **B213**, 545(E) (1983); **B194**, 445 (1982).
[20] P. J. Rijken and W. L. van Neerven, Nucl. Phys. **B487**, 233 (1997); Phys. Lett. B **386**, 422 (1996); A. Mitov and S. O. Moch, Nucl. Phys. **B751**, 18 (2006).
[21] G. Curci, W. Furmanski, and R. Petronzio, Nucl. Phys. **B175**, 27 (1980); W. Furmanski and R. Petronzio, Phys. Lett. **97B**, 437 (1980); L. Beaulieu, E. G. Floratos, and C. Kounnas, Nucl. Phys. **B166**, 321 (1980).
[22] M. Stratmann and W. Vogelsang, Nucl. Phys. **B496**, 41 (1997).
[23] S. Moch and A. Vogt, Phys. Lett. B **659**, 290 (2008).
[24] M. Stratmann and W. Vogelsang, Phys. Rev. D **64**, 114007 (2001); D. de Florian, R. Sassot, M. Stratmann, and W. Vogelsang, Phys. Rev. Lett. **101**, 072001 (2008); Phys. Rev. D **80**, 034030 (2009).
[25] A. Daleo, D. de Florian, and R. Sassot, Phys. Rev. D **71**, 034013 (2005); A. Daleo and R. Sassot, Nucl. Phys. **B673**, 357 (2003); A. Daleo, C. A. Garcia Canal, and R. Sassot, Nucl. Phys. **B662**, 334 (2003).
[26] F. Aversa, P. Chiappetta, M. Greco, and J.-Ph. Guillet, Nucl. Phys. **B327**, 105 (1989); D. de Florian, Phys. Rev. D **67**, 054004 (2003); B. Jäger, A. Schäfer, M. Stratmann, and W. Vogelsang, Phys. Rev. D **67**, 054005 (2003).
[27] A. D. Martin, R. G. Roberts, W. J. Stirling, and R. S. Thorne, Eur. Phys. J. C **28**, 455 (2003).
[28] V. Guzey, M. Strikman, and W. Vogelsang, Phys. Lett. B **603**, 173 (2004).
[29] D. de Florian, M. Stratmann, and W. Vogelsang, Phys. Rev. D **57**, 5811 (1998).
[30] FORTRAN codes of the obtained parametrizations are available upon request from the authors.